

RESEARCH

Open Access



# Susceptibility areas identification and risk assessment of debris flow using the Flow-R model: a case study of Basu County of Tibet

Huang Xu<sup>1,3</sup>, Peng Su<sup>1</sup>, Qiong Chen<sup>1,2\*</sup>, Fenggui Liu<sup>1,2</sup>, Qiang Zhou<sup>1,2</sup> and Linshan Liu<sup>3</sup>

## Abstract

**Background:** Uncertainties exist in the magnitude and outbreak of debris flow disasters, resulting in significant loss of lives and property to human society. Improved identification of debris flow susceptibility areas can help to predict the location and sphere of influence of debris flow disaster, thus accurately assessing the risk of debris flow disaster and reducing losses caused by such a disaster. The dry-hot valleys of Basu County in the Eastern Qinghai-Tibet Plateau are typical areas of high debris flow incidence, mapping of debris flow susceptibility identification and regional risk assessment is needed in this area.

**Results:** The parameters improved Flow-R model was first applied to identify debris flow susceptibility areas in Basu county using the digital elevation model, flow accumulation, slope, plan curvature, and land use data, followed by debris flow risk assessment. The Flow-R model can output high result accuracy of high-resolution susceptibility to debris flow identification on a regional scale with less data, and its accuracy value is 87.6%, indicating that the susceptibility to regional debris flow disaster is credible. This study provides a useful basis for effective prevention of regional debris flow disasters in the future, and provides a useful method for effectively identifying the debris flow susceptibility areas and assessing the related risk in large-scale areas.

**Conclusions:** (1) The debris flow susceptibility areas in Basu County covered 97.04 km<sup>2</sup> (0.79% of the study area), distributed mainly in the Nujiang River Valley, Lengqu tributaries, and both sides of National Highway 318. (2) The debris flow susceptibility areas were dominant in zones characterized by an altitude range of 3000–4000 m, a plane curvature of  $-2/100\text{ m}^{-1}$  to  $1/100\text{ m}^{-1}$ , and a low slope of 20°–40°. In addition, the susceptibility areas were dominant in the unused land and less prevalent in the water area. The highest and lowest susceptibility values were observed for cultivated and unused lands, respectively. (3) The debris flow risk in the study areas accounted for 0.82 km<sup>2</sup> and revealed a distribution of high-risk debris flow along roads. The areas with a high debris flow risk were mainly distributed along the mainstream of the Nujiang River, which is the main future protected area.

**Keywords:** Flow-R model, Debris flow, Susceptibility areas, Basu County

## Introduction

Debris flow is a common geological disaster in mountainous areas, with complex causes and high suddenness. Under favorable terrains, high loose materials and water amounts flow through gullies under the force of gravity, damaging the surrounded traffic roads, buildings, vegetation, and cultivated lands (Iverson 1997; Tang and Liang 2008). Every year, debris flows cause thousands of deaths and huge economic losses worldwide (Dowling and Santi

\*Correspondence: qhchenqiong@163.com

<sup>1</sup> College of Geographic Sciences, Qinghai Normal University, Xining 810008, China

Full list of author information is available at the end of the article

2014). China is one of the countries where debris flow disasters are most severe. Indeed, about 2/3 of the mountainous areas in China are affected by debris flow (Cui et al. 2000). Hengduan, in the southeast of the Qinghai-Tibet Plateau, is a mountainous area characterized by high mountains, intense tectonic activity, complex and diverse geological and geomorphological environment, vagaries of climate and concentrated precipitation time, and frequent mountain disasters. According to Bian et al. about 932 mountain disasters occurred in this region from 2006 to 2015, causing 1,373 casualties and 2.5 billion yuan in direct economic losses, constituting a serious threat to the safety of human life and property in this region (Bian et al. 2018). With the frequent occurrence of extreme rainfall events caused by global climate change, the frequency, scale, and complexity of debris flow in mountain areas may continue to increase in the future, presenting an increased risk of debris flow disasters (Cui et al. 2015, 2019). Therefore, accurate identification of the location, path, and extent of potential debris flow disasters can help in effective debris-flow monitoring and implementation of policies, which are crucial for accurate risk assessment of debris flow disasters. Moreover, they can also help in implementing specific and effective protective measures to, directly or indirectly, reduce or prevent losses caused by debris flow disasters.

Identification of areas susceptible to debris flows is an important approach for qualitative and quantitative assessment of the potential regional debris flow disasters (Fell et al. 2008). Susceptible areas are more likely to experience debris flow events. However, it doesn't necessarily imply a higher frequency of occurrence. Regional susceptibility mapping allows determining the spatial distribution of debris-flow risk with fewer data requirements based on DEM (Horton et al. 2013). It is usually relatively difficult to identify the site of a debris flow disaster using ground surveys (Cama et al. 2017). Therefore, combining debris flow source area detection with debris flow spread prediction is a fast and effective method to assess regional debris flow susceptibility (Horton et al. 2011; Pastorello et al. 2017). There are numerous methods for assessing debris flow susceptibility. Traditional methods are based on field disaster investigation, quantitative statistical analysis using mathematical models, and qualitative analysis (Xu et al. 2013; Kritikos and Davies 2015; Wang et al. 2017; Xia et al. 2017; Wu et al. 2019). In addition, several researchers have assessed the debris flow susceptibility using machine learning algorithms (Zhang et al. 2019; Hu et al. 2019; Xiong et al. 2020), while others have combined factors determining debris flow susceptibility in empirical models (Gomes et al. 2013; Blais-Stevens and Behnia 2016; Gong et al. 2017; Kang and Lee 2018). Compared with empirical models, mathematical

models requires extensive field survey data, which are costly and difficult to obtain, particularly at a regional scale. Although machine learning techniques can be used to assess debris-flow susceptibility at regional scales, but the model is complex to build, extremely dependent on the quantity and quality of data, with some uncertainty in weight assignment, and the training samples need to be representative, etc. their results may be inaccurate as they are incapable of differentiating susceptibility within the same debris flow gully (Qing et al. 2020). The Flow-R model is a software model for automatic identification of debris flow source areas and estimation of debris flow spread based on GIS tools. Indeed, this model can run using fewer data requirements (Horton et al. 2008, 2011). It is not an encapsulated model, and users can adjust its algorithms and parameters according to the characteristics of the study area, achieving good results. In addition, the fewer data input requirements allow for carrying out a regional-scale assessment before the occurrence of debris flow disasters (Llanes 2016; Sturzenegger et al. 2019). Numerous studies have applied the Flow-R model in debris flow assessment and showed satisfactory results (Blahut et al. 2010; Baumann et al. 2011; Horton et al. 2013; Blais-Stevens and Behnia 2016; Park et al. 2016; Kang and Lee 2018). These studies mostly compared different data resolutions, methods, and parameters, compare the susceptibility values and ranges under different parameter configurations. However, in China, relevant studies on this model have only been carried out in a few debris flow gullies (Hou et al. 2019; Nie and Li 2019). Thus, its applicability needs further exploration.

Due to the complexity of debris flow, high precision regional scale susceptibility identification research methods, large amount of demanded data, not easy to obtain, long calculation time and other limitations, regional scale susceptibility research results are often low resolution, and some high resolution data are only applicable to small regional scale. The Flow-R model is fast and efficient, with a small amount of data input to obtain debris flow susceptibility, and is more suitable for application at a large scale. Previous studies related to Flow-R model mostly compare the threshold results of different parameters at a small scale, and rarely attempt the susceptibility results at a large regional scale. In this study, Basu County of Tibet was selected as the study area. It is located in the West Hengduan Mountain area, susceptible to the occurrence of natural debris flow disasters. The Flow-R model was used to determine the identification index threshold of critical conditions, such as sediment availability, water input, and terrain slope, followed by identifying the debris flow susceptibility in the study area using the flow spreading algorithm and energy calculation of motion simulation, and an attempt is made to provide higher

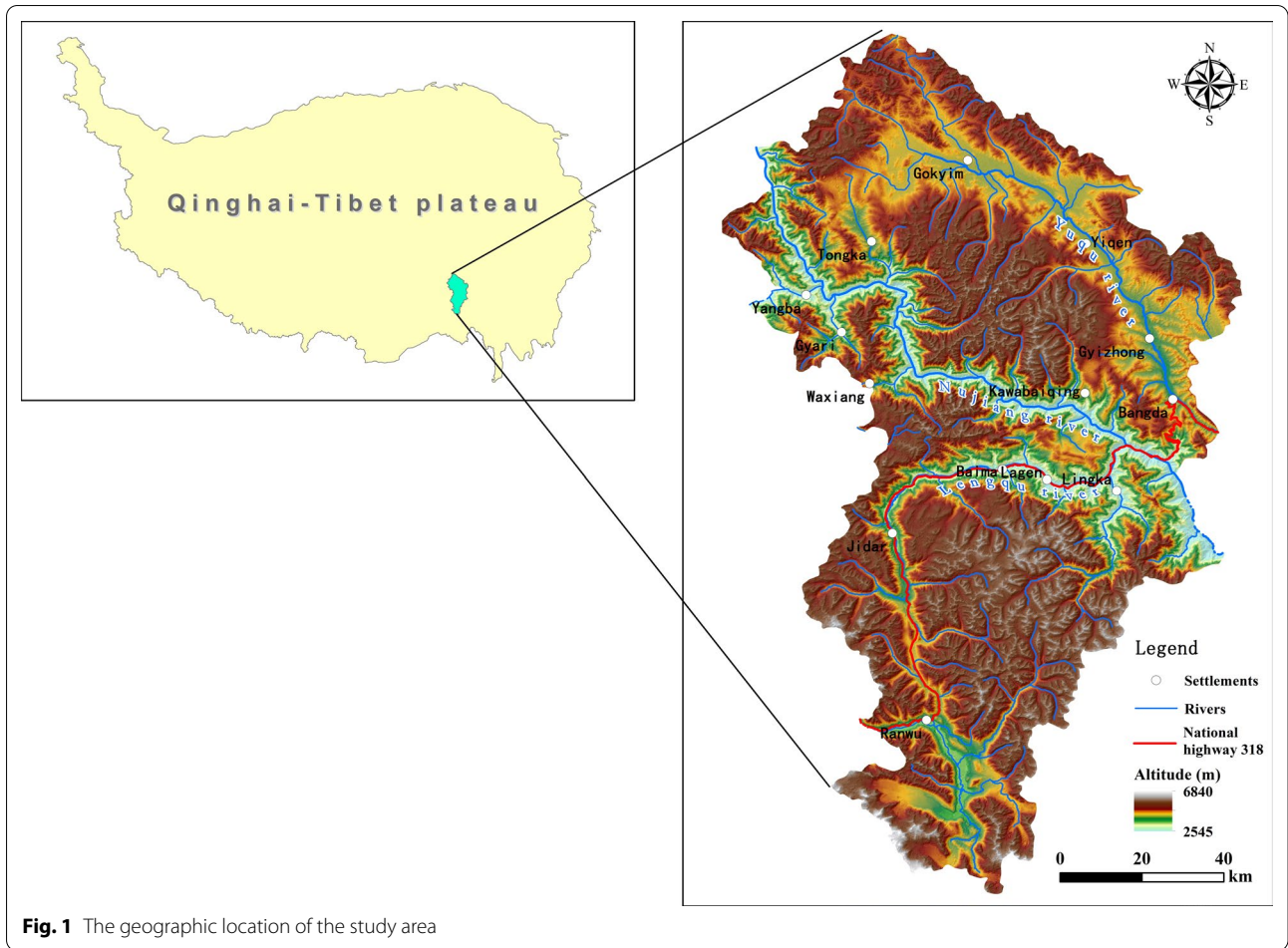


**Fig. 1** The geographic location of the study area

resolution susceptibility mapping results while selecting a large regional scale, which is representative and at the same time the results are applied to regional risk assessment, providing a reference for the future development of regional debris flow disaster prevention and control strategies.

**Study area**

In this study, Basu County of Tibet was selected as the study area. Basu county of Qamdo city is located in the southwest of China, the southeast of the Tibetan Plateau, and the west of the Hengduan mountains, covering an area of  $1.23 \times 10^4 \text{ km}^2$ , with an average altitude of around 4640 m (Fig. 1). In terms of the geological structure, the northern, central, and southern parts of the study area belong to the patchwork area of the Leiwuqi terrane, Jiayuqiao terrane, and Gangdisi massif, respectively. In addition to the high degree of metamorphism, the study area is characterized by complicated geological structures with developed fold fractures and outcropped strata. The highest elevation of the region is 6840 m, and the lowest

elevation is 2545 m, the terrain in the northeastern is high, while in the southwestern part is relatively low. It can be divided into three different geomorphic structure regions: Northwestern Plateau, Central Nujiang deep cut, and Southeastern high mountain wide valley regions (Local Chorography Compilation Committee of Basu County, 2012).

Due to the complicated geological tectonic movement and the heavy erosion by surface water, rivers are gathered in the study area. Consisting of three major river systems, namely Nujiang River, Yuqu River, and Lengqu River, with over 100 tributaries. The rivers are recharged mainly from rainfall and snow meltwater. On the other hand, the region is dominated by a temperate semi-arid plateau monsoon climate, with an average annual precipitation of 254.5 mm and an average annual amount of rainy days of 75 days, and high evaporation, with an average annual evaporation of 3000 mm. Precipitation is mainly distributed from May–September every year, accounting for 70% of the annual precipitation. The climate in the winter and spring seasons is cold and dry,

with limited precipitation, while in summer and autumn, temperature and rainfall increase as a result of southwest monsoon influence. The average annual temperature in the county and valley is 10.4 °C, while that in the alpine region is below 3 °C, the temperature is low throughout the year. Due to the dual effects of regional climate and geomorphic conditions, the overall vegetation coverage in the region is low, showing significant vertical terrain characteristics. From the valley to the plateau, the sequence of major land cover types are as follows: dry-hot valley temperate steppe, temperate meadow steppe, mountain meadow, subalpine meadow, dark coniferous forest (dominated by western Sichuan spruce), alpine meadow, alpine shrub meadow, alpine sparse vegetation, alpine sub-ice and snow, and ice and snow (Local Chorography Compilation Committee of Basu County 2012).

On the other hand, the complex and diverse topographic and geomorphologic features of the region have significant effects on the redistribution of water and heat conditions. The Foehn effect is very common in some deep gorge areas (Local Chorography Compilation

Committee of Basu County 2012), where very typical dry and hot valleys are developed. Due to the restriction of the natural environment, Basu County is sparsely populated (about 40,000 people), with a low level of social and economic development, focusing on agriculture and animal husbandry activities. In addition, the Sichuan-Tibet Line, which is a famous tourist transport line in China, passes through Basu County.

**Characteristics of the regional debris flow disaster**

The neotectonic movement in the study area is strong, with high and marked elevation differences between mountains. Indeed, the study area is characterized by complex typical deep-cut valleys, with unstable precipitation and glacier movement effects, intense erosion from the crisscrossing rivers, a large longitudinal drop of the gully bed, and steep terrain. All these characteristics contribute to the occurrence of geological disasters (eg., mountain collapse, landslide, and debris flow), threatening the safety of residents and traffic roads (Fig. 2). The area presents a high risk of debris flow development. Indeed, the area is located



**Fig. 2** Photographs of debris flows in the the study area (upper left: 29° 59' 15.81" N, 97° 10' 55.78" E; Upper right: 30° 3' 37.09" N, 96° 54' 50.61" E; Lower left: 30° 2' 20.89" N, 96° 45' 10.50" E; Lower right: 30° N, 1' 38.77" 32.90" 7' 97° E)

in a relatively complicated plot split zone, with developed fold fracture. The geological structure results in joints and fissures development, breaking up rocks. In fact, poor mechanics proprieties of rock mass result in weak weathering resistance, forming a large amount of rock debris in the gully under the influence of gravity. In addition, the region belongs to the transition zone of the southeast edge of the Tibetan Plateau, where river erosion is heavy. In the region, gullies are well developed, while valley slopes are steppe and unstable. Collapse, landslide, and rockfall occur frequently, forming a large deposit amount. Besides the low vegetation cover in the valley, caused by the Foehn effect and dry-hot climate, that contributes to debris flows, the extremely low temperatures in the high mountain areas significantly promote the freezing-thaw weathering process. The bare rock of mountains consists of a large number of detrital materials (e.g., forming rock-flowing hillsides, stone curtains, and Stone River), which transport a large amount of rock detrital materials to the gullies and provide a large number of loose detrital materials (Lv et al. 1999).

On the other hand, unstable meteorological conditions and snow meltwater in this region provide water source conditions for debris flow disasters. The annual and inter-annual precipitation in the study area is extremely variable. Along with concentrated precipitation during the flood season, most debris flow disasters occur frequently over several months. According to the climate station information of Basu County from 1980 to 2002, the maximum monthly precipitation (183 mm) was observed in July 2002, while the longest continuous rainfall duration is 11 days, and the maximum daily precipitation is 71.1 mm (October 4, 1993). The maximum (375 mm) and minimum (105.8 mm) annual precipitations were observed in 1990 and 1983, respectively. The precipitation fluctuations can significantly promote debris flow

events. Glaciers and snow cover are widely distributed in high, extremely high, and plain mountains of the study area. Indeed, with seasonal change and global warming, a large amount of water is produced by intensified snow and ice melt processes, thus increasing the debris flow disaster risk (Lv et al. 1999).

Due to the complexity of the regional terrain, canyon development, rock metamorphism, mountain fragmentation, sparse vegetation, loose soil, unstable precipitation, and snow and ice melt processes, this region provides a natural disaster-prone environment for debris flow (Lv et al. 1999). The residual slope gravel, glacial till, and drift pebble soils with poor stability are accumulated, along with water movement through the slope gradient, at the foot of the slope, the bottom of the mountain, and the outlet of secondary gullies, resulting in debris flow event. The debris flow types in this region include precipitation and glacial debris flows, with a prevalence of the precipitation debris flow type. Glacial debris flow occurs mainly in the quaternary erosion gully area of high-altitude mountains. Debris flow gullies are mostly pear-shaped, scoop-shaped, and fan-shaped, with small to medium scale.

Debris flow disaster in this region not only threatens the safety of residents but also the National Highway 318, which passes through the study area. Indeed, debris flows often destroy roads and form roadblocks (Luo et al. 1996), making this area one of the most endangered sections of the National Highway 318 (Yang et al. 2012).

## Data and methods

### Data source

Obtaining debris flow susceptibility data needs and data accessibility according to Flow-R model, the data used in this study consist of geographic information, remote sensing image, and ground survey data (Table 1). Geographic information data includes 12.5 m × 12.5 m

**Table 1** Data source

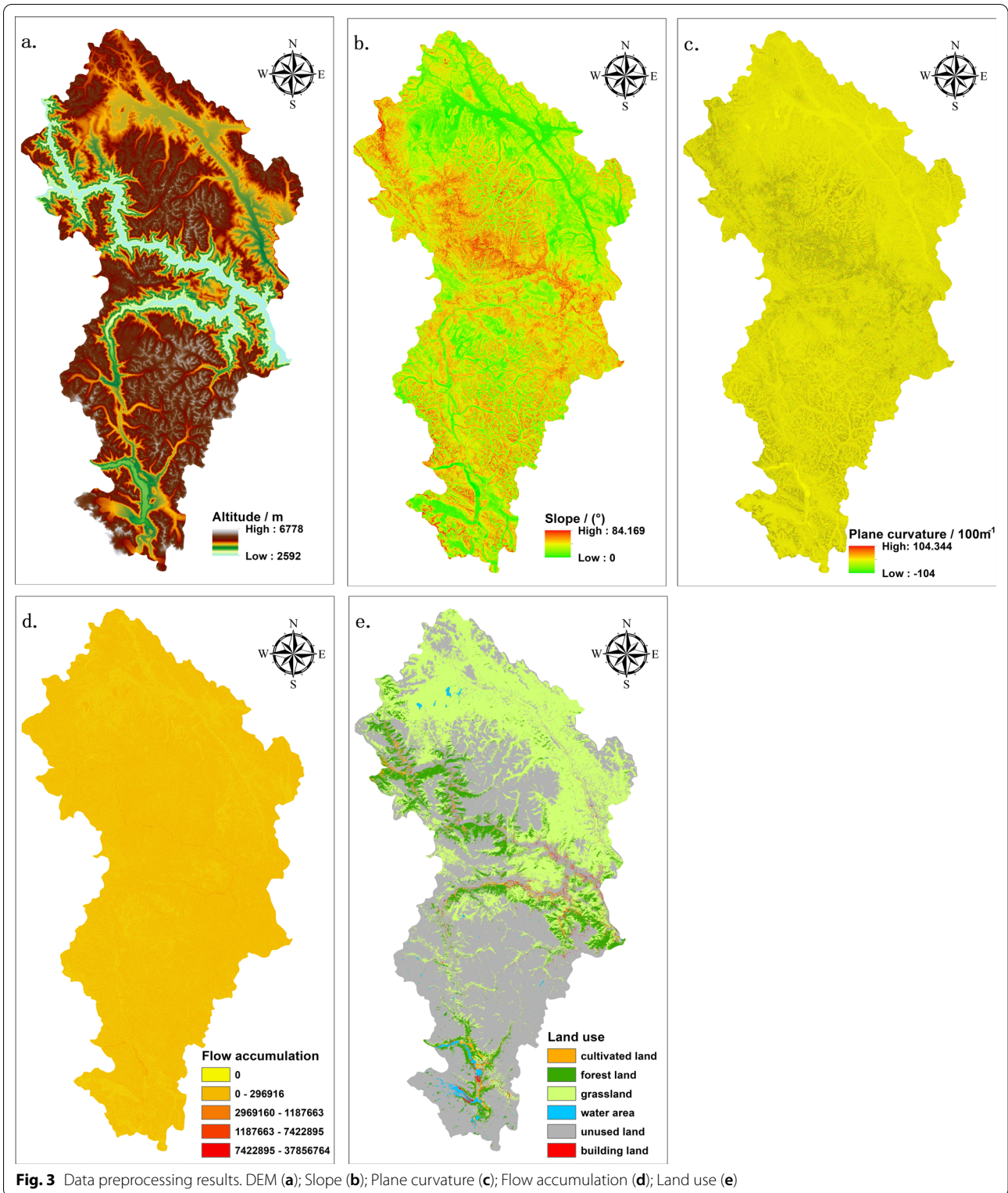
Data type	Source	Data resolution
DEM	ALOS PALSAR <a href="https://asf.alaska.edu/data-sets/derived-data-sets/alos-palsar-rtc/alos-palsar-radiometric-terrain-correction/">https://asf.alaska.edu/data-sets/derived-data-sets/alos-palsar-rtc/alos-palsar-radiometric-terrain-correction/</a>	12.5 m*12.5 m
Land cover data	Global land cover map data products <a href="http://data.ess.tsinghua.edu.cn/">http://data.ess.tsinghua.edu.cn/</a>	10 m*10 m
Spatial distribution of disaster points	Data Center for Resources and Environmental Sciences, Chinese Academy of Sciences <a href="http://www.resdc.cn/">http://www.resdc.cn/</a>	–
Landsat-8 OLI remote sensing image	USGS <a href="https://earthexplorer.usgs.gov/">https://earthexplorer.usgs.gov/</a>	30 m*30 m
Building information	OpenStreetMap <a href="https://www.openstreetmap.org">https://www.openstreetmap.org</a>	–
2020–2021 Field survey data	Debris flow disaster site	–

Digital Elevation Model (DEM), flow accumulation, slope, plan curvature, land use with 10 m × 10 m resolution, reclassification of land cover data based on different land use patterns as land use input. Building information obtained from Map street, while remote sensing image data include Landsat-8 OLI remote sensing images, with 30 m of resolution. The ground survey data consist of geological disaster information of the study area and the geological disaster data obtained during two field investigations in the 2020–2021 period.

#### Data preprocessing

DEM, flow accumulation, slope, plan curvature, and land use data were processed in ArcGIS software. DEM data were obtained by advanced land observing satellite phased array type L-band synthetic aperture radar (ALOS PALSAR) dataset, with a data resolution of 12.5 m. These data were used to determine flow accumulation, slope, and plane curvature data in ArcGIS10.2 software. In addition, land use data were obtained by processing the 2017 global land cover mapping performed by Gong et al. (2019).

1. For DEM processing, 15 scenes of images within the study area were downloaded from the website and combined under the same projection condition (The output projection coordinate system is set to: 'WGS\_1984\_UTM\_Zone\_47N' according to the zone location): According to the properties of the first scene of the image, mosaic of all 15 scenes of DEM data, with consistent attributes, the study area DEM is cropped according to the zone extent and projections to facilitate further computation and use.
  2. Slope refers to the degree of steepness of the ground surface. The slope is defined as the ratio of vertical height to horizontal distance. In this study, the slope tool was used in Arcgis software to obtain: the elevation value matrix was calculated using the DEM data synthesized, and then the slope was obtained from the proximity matrix. The slope of the study area ranges from 0° to 84.169°.
  3. Flow Accumulation refers to the accumulated flow at each point of the regional terrain, which can be obtained by the flow simulation method on the regional terrain surface. In this study, the Fill tool was used in Arcgis software to fill the pits first, and then the Flow Accumulation tool was used to obtain: the elevation value matrix was first calculated using the synthetic DEM data, and then the adjacent matrix was used to calculate the slope value and the accumulation direction. The flow direction was derived from the maximum values of the calculated slope in the eight directions, with a range value of 1–128.
- Afterward, the cumulative vectorial value of the flow was obtained by solving multiple equations. The cumulative vectorial values in the study area ranged from 0 to 37856764.
4. Plane curvature refers to the direction perpendicular to the maximum slope. Plane curvature is related to the convergence and dispersion of the flow through the ground surface. In this study in Arcgis software using Curvature tool to obtain: the slope of each grid was first calculated by referring to the adjacency matrix using DEM data, and then the second derivative of the slope was calculated by fitting the pixel with eight adjacent pixels to determine plane curvature. Positive and negative values of plane curvature indicate that the surface of the pixel is convex upward and concave upward, respectively. The plane curvature of the study area ranges from  $-104/100$  to  $104.344/100 \text{ m}^{-1}$ .
  5. In order to obtain an accurate land use map of the study area, the 2017 global land cover data, developed by Gong et al. were considered in this study. Two scenes of images of the study area were first mosaicked under the same projection (WGS\_1984\_UTM\_Zone\_47N), and then reclassified 10 land cover types based on the corresponding attribute table using the Reclassify tool in Arcgis software. The wetland, tundra/shrub, and bare/glacier snow lands were classified as water, grassland, and unused land, respectively, while other land types remained unchanged. In total, six types of land use data were obtained, namely cultivated land, grassland, forest land, artificial surface, water area, and unused land. Use resample tool to convert 10 m higher resolution to lower 12.5 m resolution, output range consistent with dem and aligned, resampling method using the default method (NEAREST).
- Through the above preprocessing, the following data results are obtained (Fig. 3):
- Regarding data fusion of geological disaster points, two geological disaster datasets were considered in this study, obtained from the data center of the Institute of Geographic Environment and Natural Resources Research, Chinese Academy of Sciences, and a field survey in the region during the 2020–2021 period. The two datasets were merged to create a new geological disaster information database. In total, 89 debris flow disaster information points were obtained in the study area.
- Remote sensing image preprocessing: In order to obtain high-resolution remote sensing images, two scenes of remote sensing images, acquired on November 17 and August 13 in 2013, with cloud covers of less than 5% were downloaded (Path/Row:134/40; 134/39). The data



processing included geometric and radiometric correction, mosaic and cropping in ENVI software, followed by the Gram-Schmidt Pan sharpening tool, sensor selection

of landsat8\_oli, and the resampling method of cubic Convolution to fuse the multispectral image (30 m) with the higher resolution panchromatic band (15 m) to obtain a

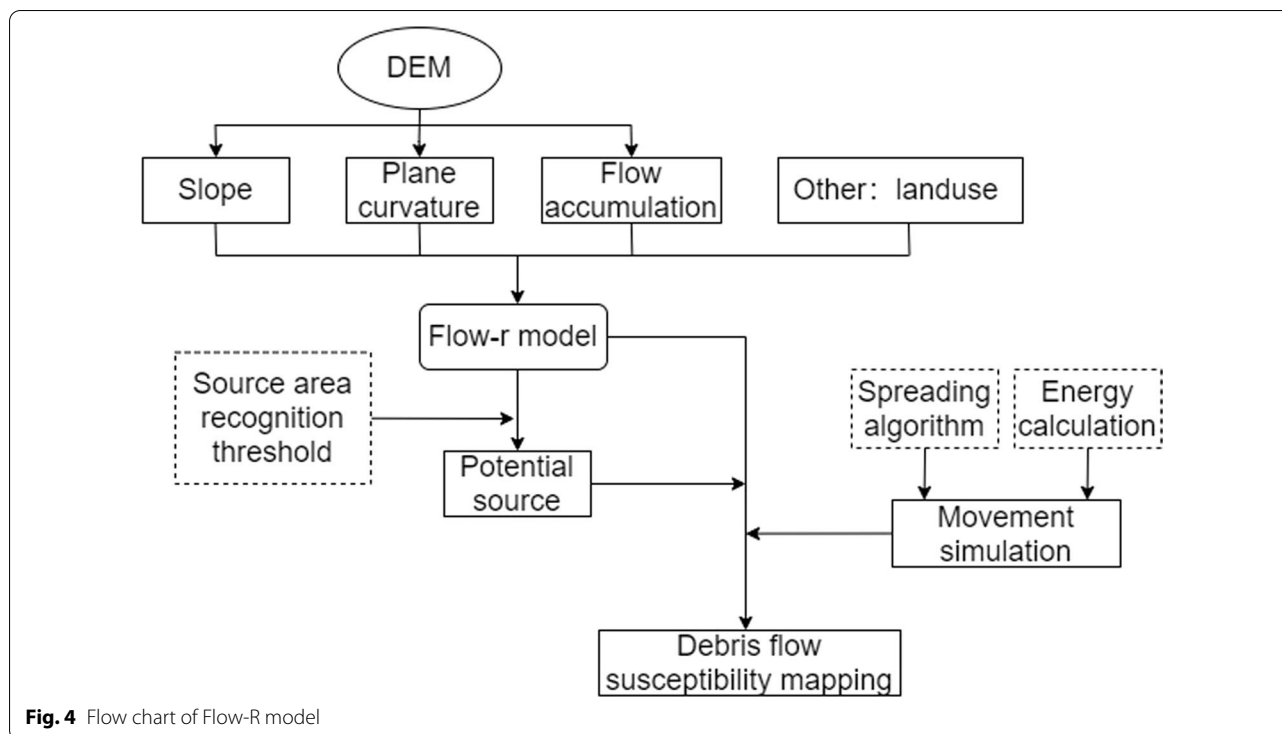


**Fig. 4** Flow chart of Flow-R model

higher resolution multispectral image with a synthetic image resolution of 15 m, acquired high-resolution remote sensing images for subsequent result validation.

**Flow-R model**

The Flow-R model is a GIS-based simulation model of regional-scale gravity disaster path, combining debris flow source area detection with debris flow spread prediction. The purpose is to locate hazardous processes and gain insight into existing or potential susceptible areas, mainly involving areas with conditions for debris flow to occur, and reflecting the extent to which debris flows may spread (Horton et al. 2008). The model was obtained from the Flow-R website of Lausanne University ([https://](https://www.flow-r.org/)

[www.flow-r.org/](https://www.flow-r.org/)). Horton et al. developed Flow-R model for disaster susceptibility identification (Horton et al. 2008), which consists of two parts: identification of the potential source area and simulation of debris flow movement (Fig. 4). The model output results in the area under the debris flow spread range and the associated qualitative probability of being vulnerable to the potential risk of debris flow, with higher values indicating a higher probability of debris flow arrival. The potential spread indicates the worst-case scenario, so the area of susceptibility results is often larger than the actual area of the site (Horton et al. 2008).

The identification of potential source area in this model is based on three critical factors of debris flow occurrence: sediment availability, water input, and terrain slope. The input variables include DEM, slope, plane curvature, and flow accumulation. Users can add lithology, elevation, surface curvature, land use variables as input, and limit source region identification conditions to improve the simulation accuracy (Horton et al. 2008). By dividing the threshold of each element for source area identification, values in the layer of each input dataset are divided into three types: source area, non-source area, and uncertain area. The potential source area of debris flow is defined as an area whose superimposed layers were divided into source areas at least once and were never divided into non-source areas.

**Table 2** Input parameters used in the Flow-R model

Parameters	Method	Value
Slope	–	15°–40°
Plane curvature	–	– 0.5/100 m <sup>-1</sup>
Flow accumulation	Rare event	10 m DEM
Direction algorithm	Holmgren (1994) modified	dh = 2 Exp = 04.0
Inertial algorithm	Weights	Gamma_2000
Friction loss function	Travel angle	11.0_deg
Energy limitation	Velocity	15_mps



The movement of debris flow is simulated using a spreading algorithm and an energy calculation. Among them, the spreading algorithm of debris flow is determined based on the flow directions algorithm and the inertial algorithm, while the energy calculation of debris flow is determined based on the friction loss function and the energy limitation. Users can select and adjust the thresholds of calculation methods and parameters provided by the model according to the requirements.

**Selection of Flow-R model parameters**

Due to the large scale of the study area and the different environmental factors driving natural disasters, global susceptibility distribution from a macro perspective was considered in this study, selecting input parameters based on data availability. Thresholds were fixed based on previous studies (Table 2).

The slope is an important factor in identifying susceptible areas to debris flow. According to previous studies, debris flow is more likely to occur under

the slope range of 15°–40° (Takahashi, 1981; Rickenmann and Zimmermann, 1993; Horton et al. 2013). The plane curvature is the curvature perpendicular to the steepest slope, and the negative value is generally the gullies prone to debris flow (Horton et al. 2013). Indeed, the value increase with increasing DEM resolution, and the values generally range from  $-2/100$  to  $0.01/100 \text{ m}^{-1}$  (Baumann et al. 2011). Park et al. used DEM with 10 m resolution and a threshold value of  $-1/100 \text{ m}^{-1}$  to achieve high accuracy of simulation results (Park et al. 2016). In this study, the DEM data resolution was 12.5 m, and the threshold value was set to  $-0.5 \text{ m}/100 \text{ m}^{-1}$ . The cumulative amount is the flow accumulation of each grid point obtained using the flow simulation algorithm.

Rare/extreme precipitation events with different resolutions can be selected in the model. The rare precipitation event algorithm was selected in this study. Geological lithology or land use data can be used as input providing provenance information (Horton et al. 2011). The geological conditions of the study area are

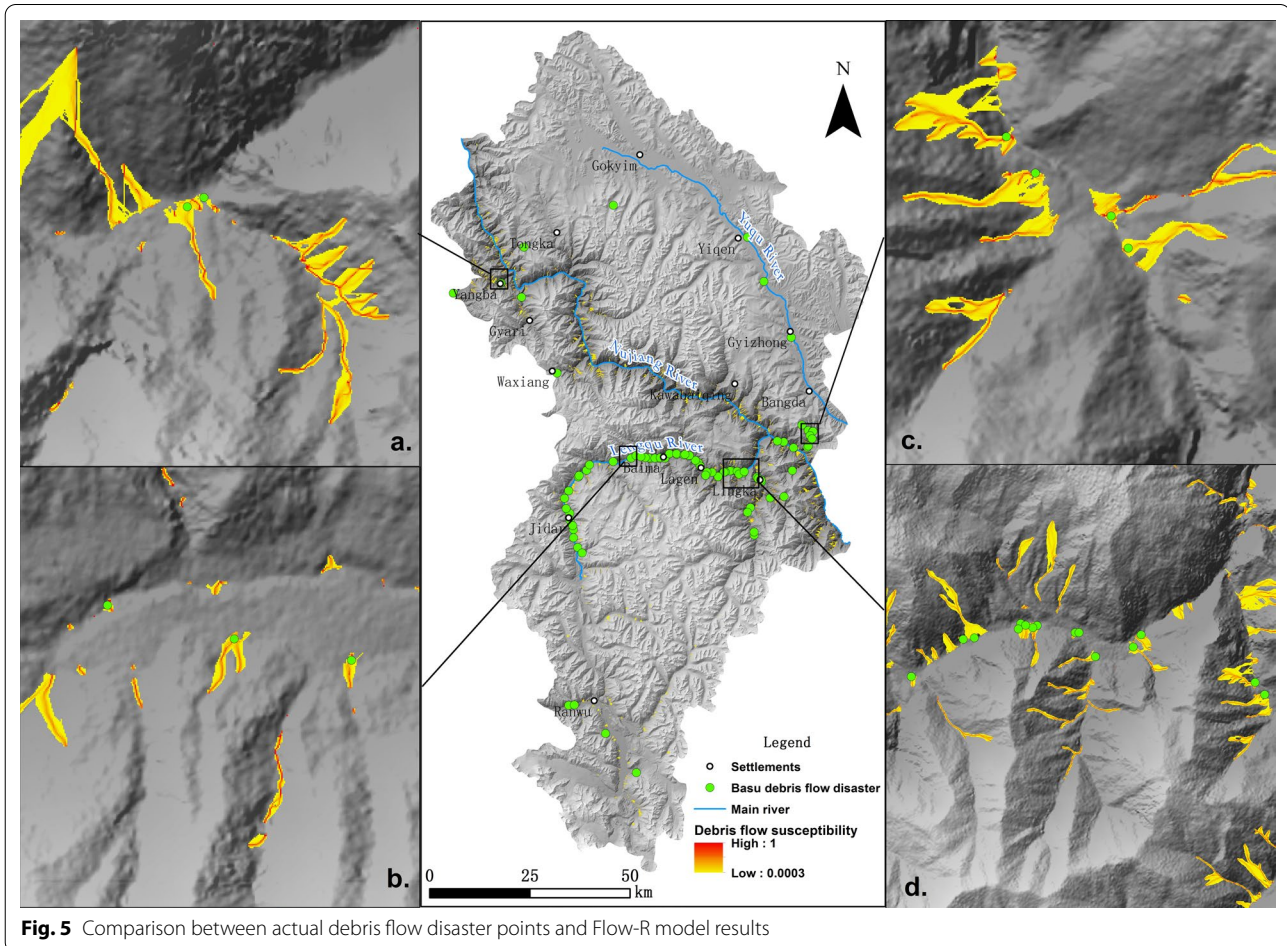


**Fig. 5** Comparison between actual debris flow disaster points and Flow-R model results

complex, while the accuracy of the publicly available geological data is low. Therefore, the geological parameter was ignored in this study, defining the geological condition of the study area as an uncertain source area. Land use data were considered to reflect provenance input conditions, according to the stability differences of debris flow under different land-use types (Xie and Wei, 2011). Indeed, water/grassland, artificial surface/cultivated land, forest/unused land were set as source areas, uncertain, non-source areas, respectively. In the Flow-R model, the flow direction algorithm, inertial algorithm, friction loss coefficient, and energy limitation method adopted parameters given by Horton et al. (2008).

**Methodology of debris flow disaster risk assessment**

Human society is the most exposed to debris flow disasters and related damage. Predicting potential debris flow susceptibility areas and combining them with exposure bodies (artificial buildings, roads...) can help managers to better evaluate hazard-affected risk. Indeed, establishing preventive strategies and implementing effective measures to reduce human activities in high-risk areas can effectively reduce the economic losses caused by natural debris flow disasters in the region (Shi 2018). In this study, the assessment of debris flow disaster risk was carried out based on susceptibility identification of debris

flow, providing targeted monitoring and early warning reference for accurate assessment of debris flow disaster risk.

Disaster risk assessment is the analysis and evaluation of life, property, livelihood, and the vulnerability of the disaster-causing factors and exposure bodies that may cause potential threats or injuries to human society. Disaster risk per unit area is closely related to disaster susceptibility and vulnerability of the body exposure within a given area, which can be obtained by combining susceptibility and vulnerability. In this study, debris flow disaster risk was determined using the following formula:

$$\text{Debris flow disaster risk} = \text{Debris flow susceptibility areas} * \text{Vulnerability of risk exposure body} \tag{1}$$

Debris flow disaster in the study area is mainly affected by roads, settlements, residential buildings, farmland, and engineering facilities. In this study, the selection of risk exposure body factors considered surface objects related to human society, including artificial buildings, roads, houses, and cultivated lands, which are often vulnerable to disaster, resulting in economic losses. Although forest, grassland, unused land, water body, and other natural environment are also vulnerable to damage, they have some capacity for self-regulation, resulting in low social and economic losses. Indeed, these land types

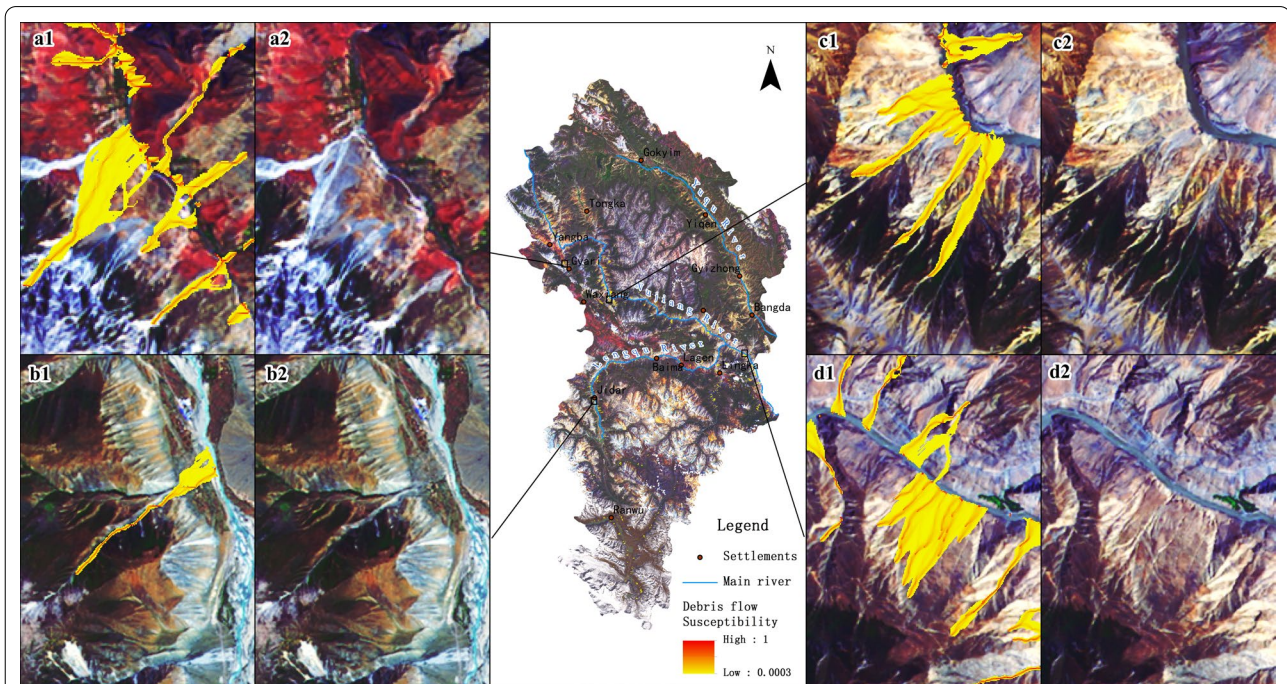


**Fig. 6** Random partial validation using Landsat-8 OLI\_TIRS images. **a1, b1, c1, and d1** represent the susceptibility results of debris flow superimposed on four remote sensing images; **a2, b2, c2, and d2** represent base maps of remote sensing images

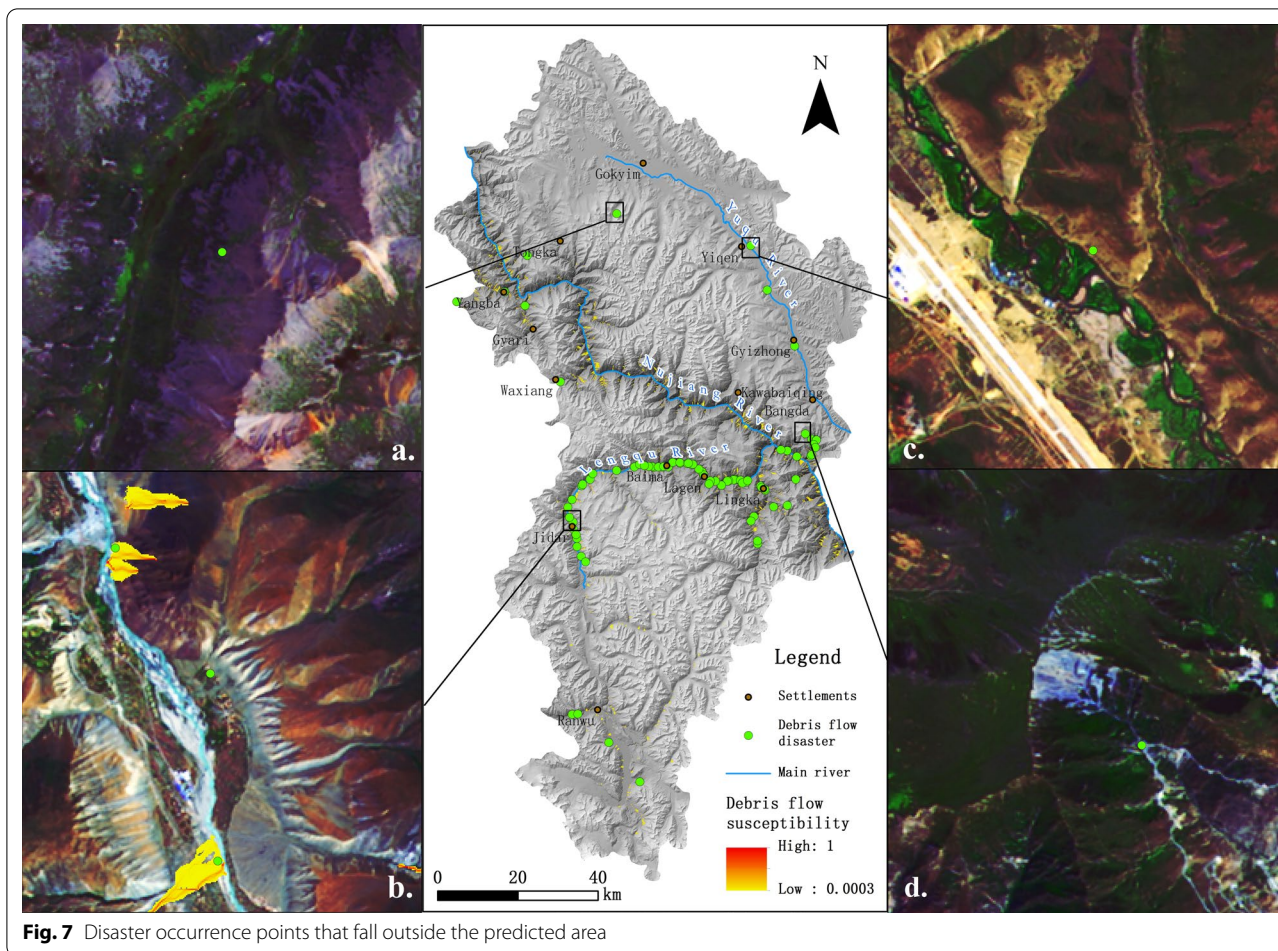


**Fig. 7** Disaster occurrence points that fall outside the predicted area

**Table 3** Data of disaster points not located in susceptibility areas

Points	Villages and towns	Longitude	Latitude
1	Gokyim	96° 46' 31"	30° 37' 15"
2	Lagen	97° 1' 51.1"	30° 1' 26.5"
3	Jidar	96° 40' 41.2"	29° 55' 34.8"
4	Baima	96° 55' 16.90"	30° 3' 13.28"
5	Tongka	96° 32' 42.48"	30° 31' 21.02"
6	Bangda	97° 16' 28.7"	30° 8' 0.7"
7	Bangda	97° 18' 11.61"	30° 7' 12.38"
8	Bangda	97° 18' 12.45"	30° 7' 11.07"
9	Gyizhong	97° 14' 35.8"	30° 19' 48.8"
10	Gyizhong	97° 10' 11.87"	30° 27' 18.8"
11	Yiqen	97° 7' 31.5"	30° 33' 16"

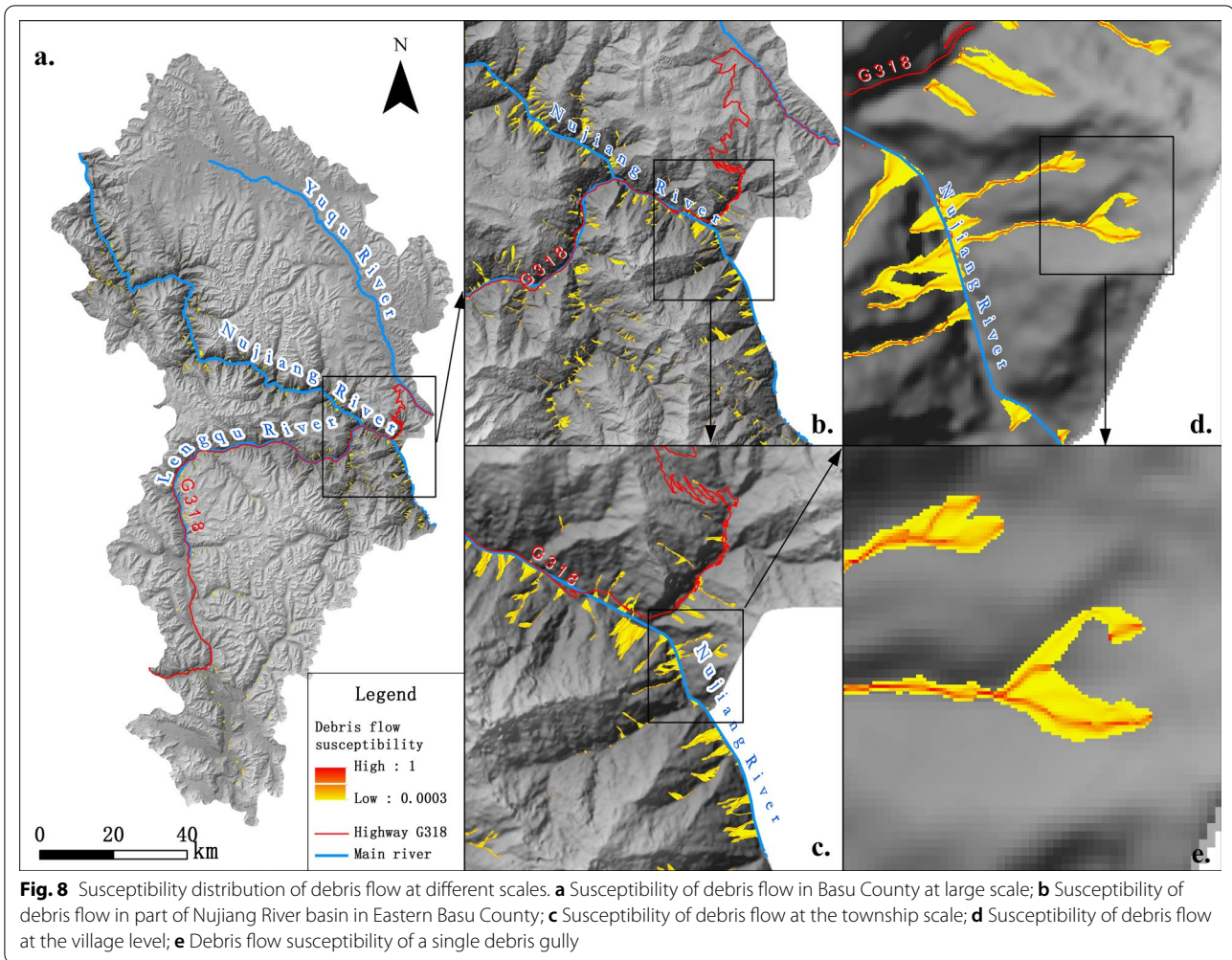
exhibit low vulnerability to flow-debris disasters. The disaster risks of artificial facilities, cultivated land, and other highly vulnerable bodies were determined to evaluate the regional debris flow disaster risk.

Bodies at risk of exposure along potential debris flow paths in the study area were identified to determine the area and extent of regional disaster risk exposure. Vector data of buildings, residential areas, agricultural lands, parks, and roads were first extracted from OpenStreet-Map data, and then the completeness of the risk exposure body at random locations was checked using Google Earth before being assessed.

## Results

### Verification of the debris flow susceptibility results

The range of susceptibility results output by Flow-R is consistent with each layer, and the data resolution is 12.5 m × 12.5 m. There are 78947809 raster cells in the study area, among which, 6211045 raster cells have susceptibility result value distribution, and the rest of the raster cells are NoData (- 9999). According to the Flow-R model results, the highest and lowest debris-flow susceptibility values were 1 and 0.0003, respectively (Fig. 5), The higher the susceptibility value, the greater the possibility of debris flow spreading, the lower the



susceptibility value, the lower the possibility of debris flow spreading, and the non-distribution of susceptibility value means that there are no conditions for debris flow disaster and the debris flow does not spread. The higher the susceptibility value, the lower the area range. In this study, the susceptibility results from the model are verified using the distribution of disaster points list data. In Arcgis software, the susceptibility results are extracted to the disaster distribution point data, and the points with susceptibility values are the correct points for the model debris flow simulation, and the points with the value of - 9999 are the wrong simulation points. The susceptibility results obtained by the model were validated using the actual debris flow disaster points (89 points). The results showed 78 disaster points in the susceptibility areas identified by the model, while 11 points were located outside the identified areas, indicating a good simulation accuracy value of 87.6%.

The actual debris flow disaster points were identified from field investigations. Thus, the number of

verification points was limited and mainly located along the highway. Indeed, some susceptibility areas identified using the Flow-R model were located on slopes and gullies at higher elevations, making it difficult to validate them using field data. Therefore, remote sensing image data were used to further verify the result. Landsat-8 OLI\_TIRS satellite remote sensing images were used to perform random local verification, the main judgment is based on whether the part with susceptibility value has almost no vegetation cover, serious surface damage, exposed soil, rough texture, irregular perimeter, inconsistent with the overall texture of the surrounding area and whether there is a formation area, circulation area, accumulation area, these debris flow traces or debris flow ditch, etc. as the basis for judging whether the results are reasonable (Fig. 6). Four groups of susceptibility areas (Fig. 6a1, b1, c1, d1) were randomly selected and compared with those identified using remote sensing images (Fig. 6a2, b2, c2, d2). The results revealed that high susceptibility areas included obvious debris flow gullies in

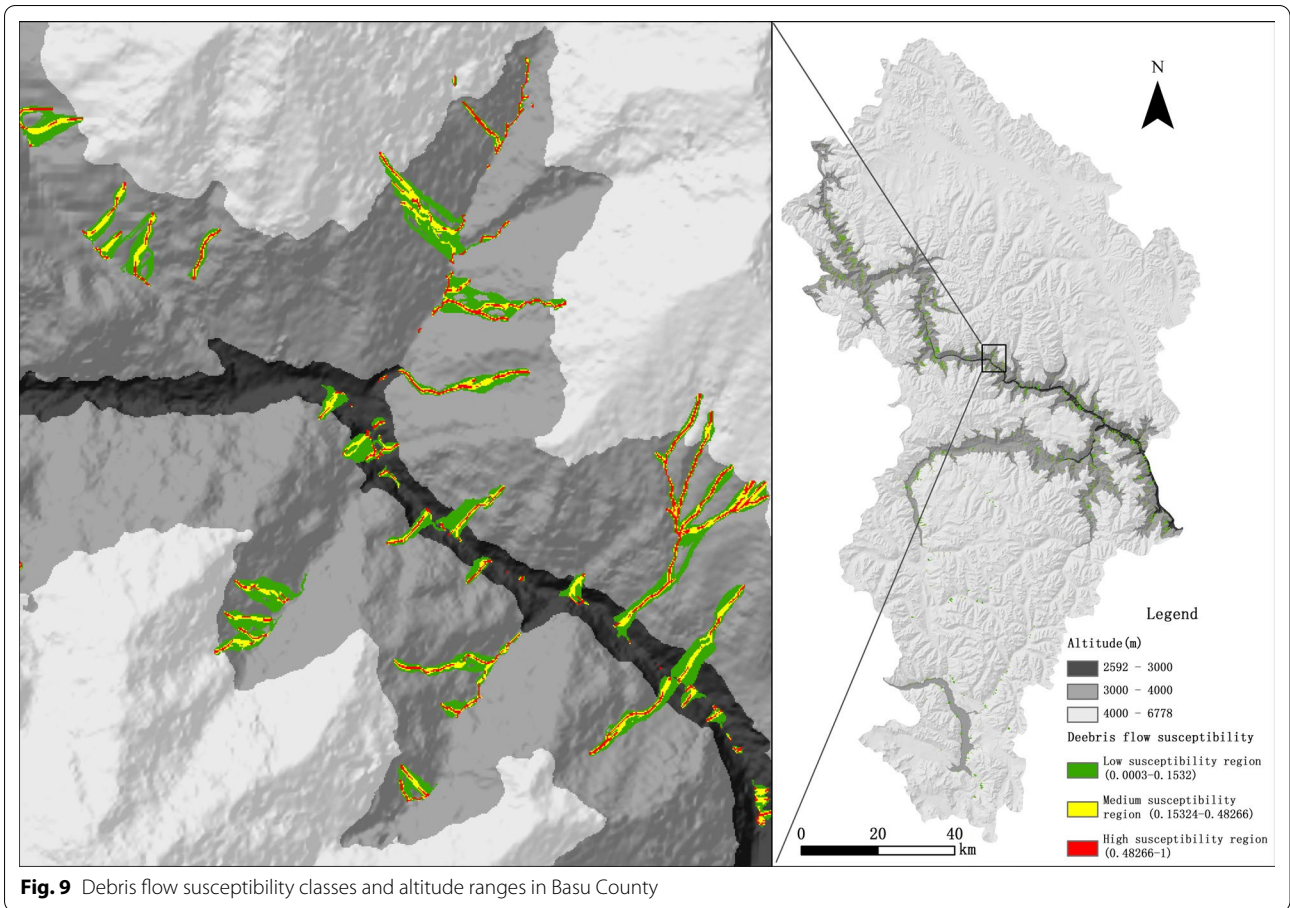


**Fig. 9** Debris flow susceptibility classes and altitude ranges in Basu County

**Table 4** Statistics of different debris flow susceptibility classes in Basu County

Type	Area/km <sup>2</sup>	Proportion of susceptibility areas of debris flow/%	Percentage of the area in Basu County/%
Low susceptibility	72.61	74.8	0.59
Medium-susceptibility	18.49	19.1	0.15
High susceptibility	5.94	6.1	0.05
Total	97.04	100	0.79

the mountain, while areas of low susceptibility exhibited scattered loose debris flow. The overall comparison and verification results suggest good simulation results.

The verification results showed 11 disaster points outside the susceptibility areas (Fig. 7 and Table 3). This finding may be due to several reasons. First, the accuracy of input data can affect the identification accuracy of the susceptible areas for debris flow, as the Flow-R is an empirical model. Second, there were 7 debris flow points in the non-susceptible areas in the tributaries of Yuqu River (points 1, 7, 8, 9, 10, and 11), with a lack of

susceptibility information near the disaster occurrences points. Indeed, by referring to the susceptibility identification results of debris flow and local Chronicles (Local Chorography Compilation Committee of Basu County 2012), it was observed that the debris flow disaster in the Yuqu river tributary basin in the study area has not developed. As the formation of debris flow disaster is complex to a certain extent, geological, lithology, soil, and other intrinsic parameters were not used to further restrict the selection of source area. Therefore, the disaster points may exhibit local favorable accumulation conditions for

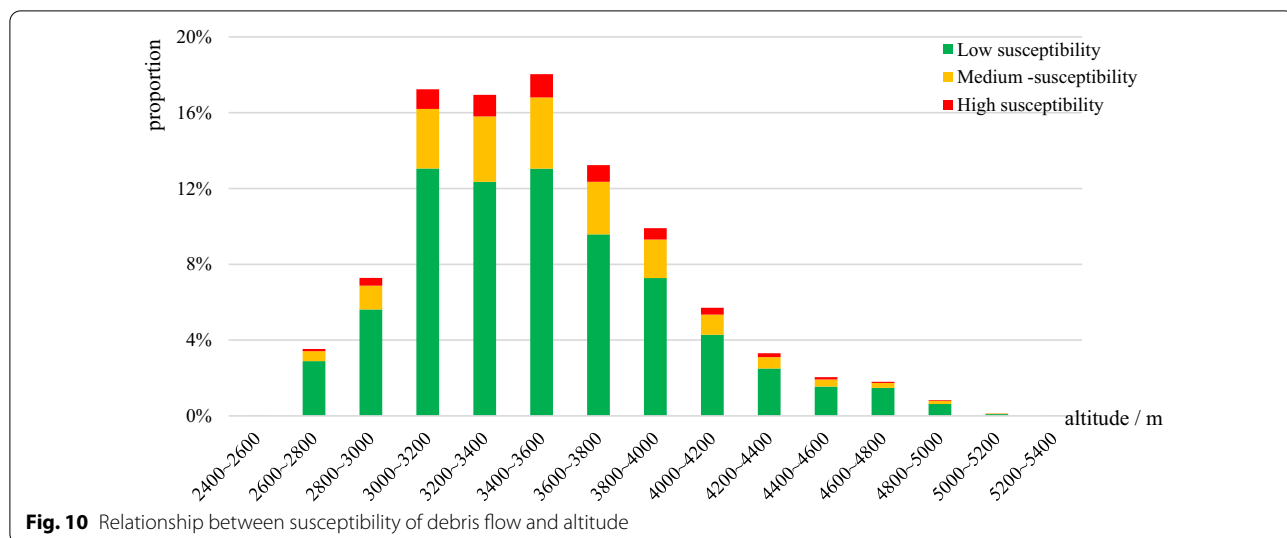


**Fig. 10** Relationship between susceptibility of debris flow and altitude

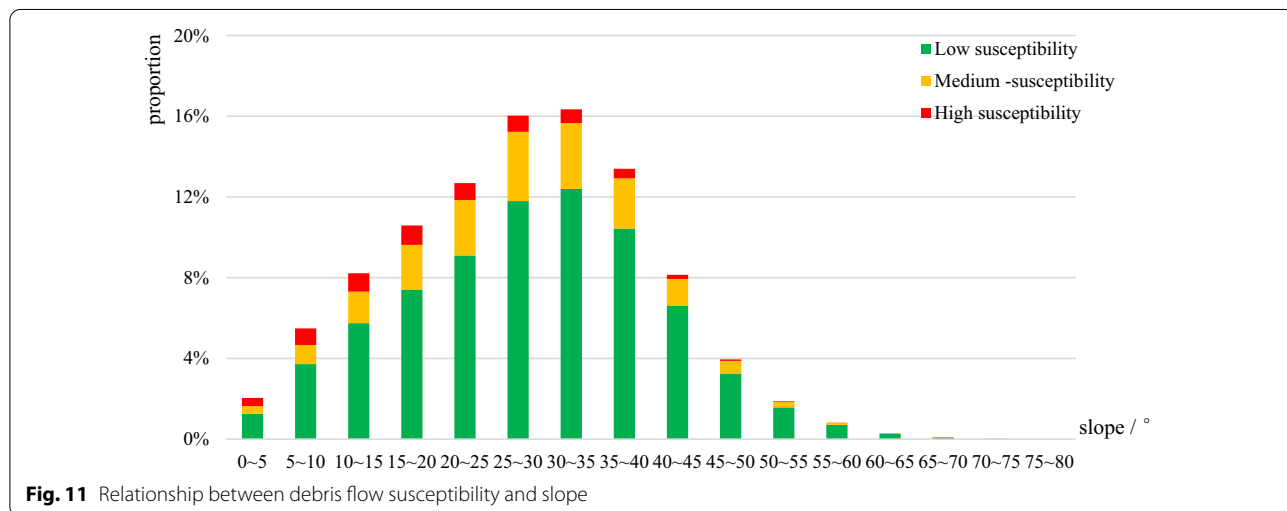


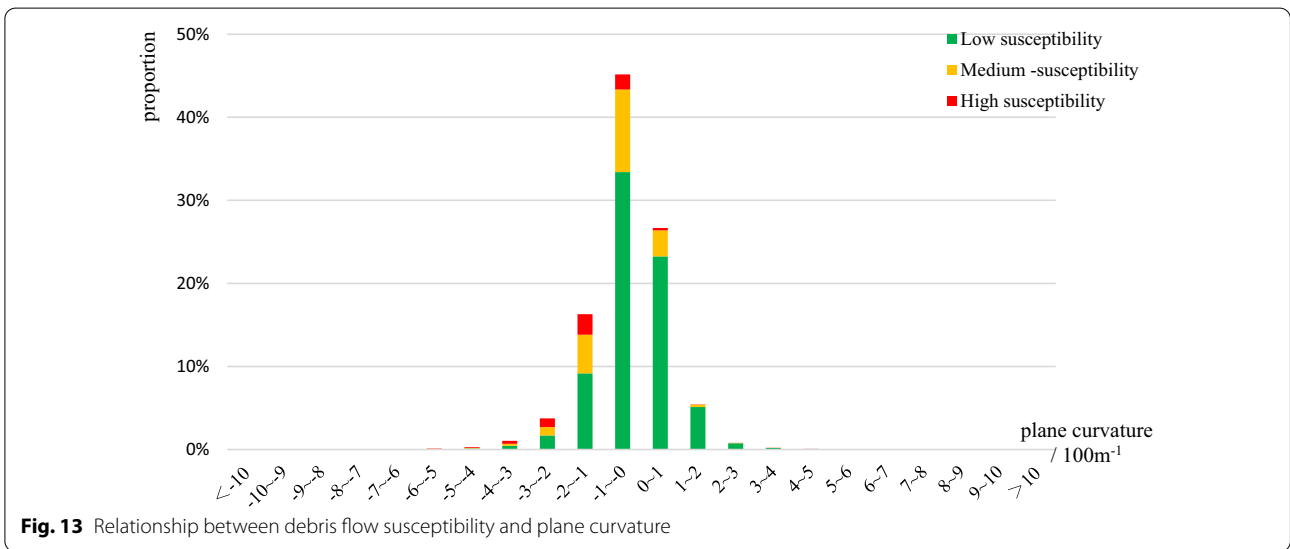
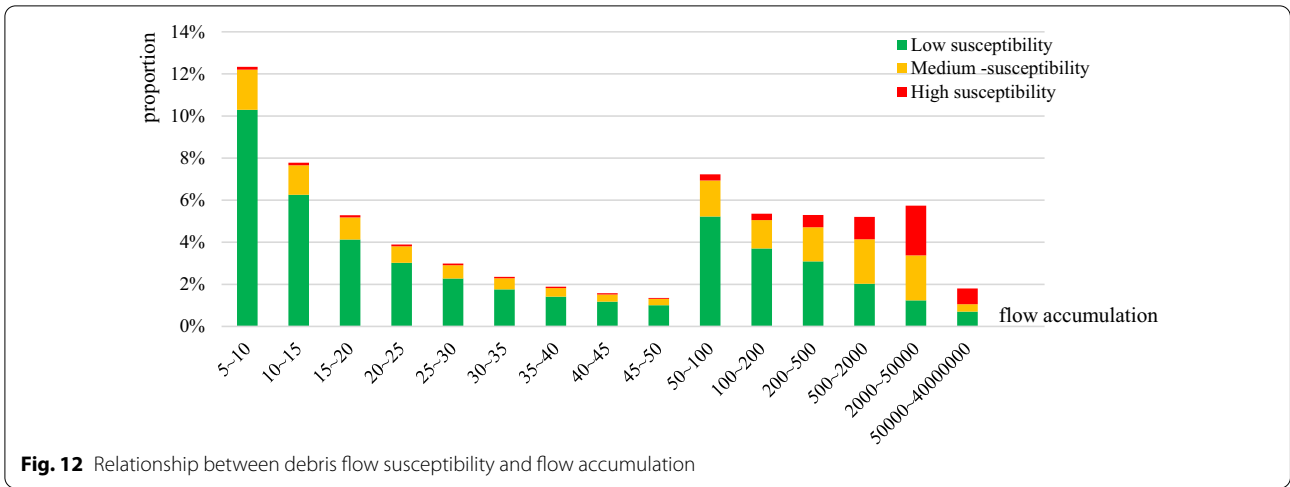
**Fig. 11** Relationship between debris flow susceptibility and slope

debris flow occurrence, forming debris flow gullies under sufficient precipitation (Fig. 7a, c, d). Third, due to the large scale of the study area and the obvious differences in the natural environment, disaster thresholds may be spatially different, resulting in discrepancies in the results. Fourth, the disaster points come from manual records, some debris flows occur in high mountains, which are observable but inaccessible, and the recorded information may not represent the exact location of the debris flow, leading to discrepancies in the results. Finally, some disaster points were recorded as hillslope debris flow (Table 3, points 3–11), while the plane curvature value was greater than the threshold set when identifying the source area, potentially causing non-identification of diffuse slopes (Fig. 7b, c).

**Susceptibility areas identification**

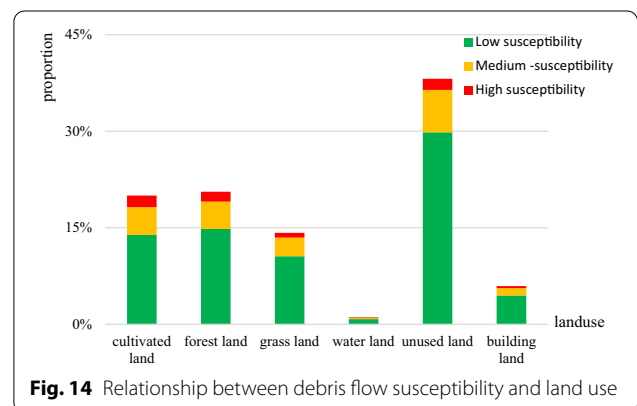
Debris-flow susceptibility mapping can help to determine and thoroughly assess the most likely affected areas by the flow debris disaster. The susceptible areas are the areas likely to be affected by debris flow disasters, which may not occur due to vegetation covering debris flow gullies. Obtaining accurate data is a labor-intensive task, making it difficult to carry out disaster identification and inspection on a regional scale.

The Flow-R model can rapidly provide the debris-flow susceptibility results at a large county scale, with fewer input data and a resolution of 12.5 m (Fig. 8). As shown in Fig. 8a, the results were not conclusive in the macroscopic scale of the study area, showing small debris-flow susceptibility areas without being able to examine the



spatial differences of susceptibility. Thus, by adjusting the scale, the distribution and differences between the flow-debris susceptibility areas were well identified (Fig. 8b–e).

National Highway 318 has great importance and influence on the development of southwest China. Previous studies on debris flow disasters in this region mainly focused on the route along Highway 318 (Zou et al. 2013), without considering other areas in the study region. In addition, most of the research results were segmented according to debris flow hazard zoning, even some areas are not at risk. Thus, these results have not revealed the change of debris flow risk in different regions at the microscale of the study area and identified the debris flow risk area for subsequent disaster



prevention and mitigation. Our study showed that the susceptibility areas of debris flow are not only distributed along National Highway 318 and Lentqu river tributary but also on both sides of Nujiang River valley. Indeed, the susceptibility areas along the Nujiang River valley are large, while no risk was observed in the adjacent Yuqu river tributary. Debris flow susceptibility areas are prone to disasters, presenting a high-risk degree with a small range, distributed mainly along the valley. While areas presenting low-risk are large, spreading around the channel depending on the terrain.

**Classification and distribution characteristics of debris flow susceptibility areas**

The debris flow susceptibility area was 97.04 km<sup>2</sup>, accounting for about 0.79% of the study area. The susceptibility results were divided into three classes using the natural breaks (Jenks) method provided In Arcgis software, namely low-susceptibility, medium-susceptibility, and high-susceptibility classes (Fig. 9).

According to the results of the Flow-R model, the spatial distribution of susceptibility classes was analyzed. The area of low susceptibility areas was about 72.61 km<sup>2</sup>, accounting for 0.59 and 74.8% of the study area and the total surface of debris flow area, respectively. The medium susceptibility area covered about 18.49 km<sup>2</sup>, accounting for 0.15 and 19.1% of the study area and the total debris flow susceptibility areas, respectively. The high susceptibility area was about 5.94 km<sup>2</sup>, accounting for 0.05 and 6.1% of the study area and the total debris flow area, respectively (Table 4). In addition, the area of medium–high susceptibility region was relatively small, which is related to debris flow circulation area. Over 70% of the areas revealed low susceptibility to debris flow, mainly in the accumulation area, which is the attenuation and diffusion zone of debris flow. Therefore, although debris flow occurs frequently in the study area, the area affected by debris flow disaster is small, while the area’s high susceptibility to debris flow accounted for a small surface.

The raster file of susceptibility results is converted into Points element shapefiles in Arcgis, and the values are extracted to points, then altitude, slope, plane curvature, flow accumulation and land use values are extracted to points, and the area is classified into different classes according to different feature values, so that the analysis can calculate the percentage of the area of different susceptibility classes in each feature class.

The results of the relationship between debris flow susceptibility and altitude (Fig. 10) show that we did not restrict the altitude at which debris flow occurs in the model, although the average altitude of the study area

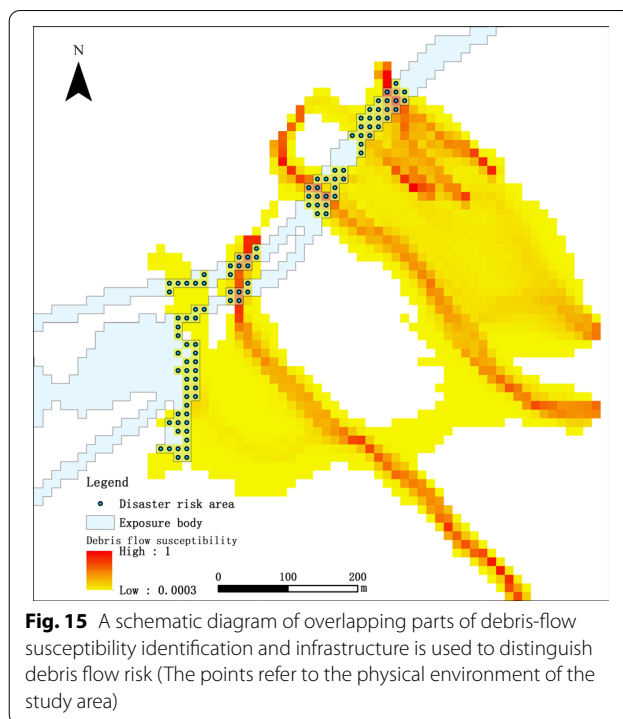


**Fig. 15** A schematic diagram of overlapping parts of debris-flow susceptibility identification and infrastructure is used to distinguish debris flow risk (The points refer to the physical environment of the study area)

reaches 4640 m, and the range of debris flow susceptibility is 2599–5279 m. The debris flow susceptibility areas are mainly distributed in the study area below 4000 m in altitude, and the distribution is more concentrated on both sides of the river valley at 3000–4000 m in altitude (Fig. 9). The results indicate that deep canyons with high elevation differences provide favorable topographic conditions for the occurrence of debris flow disasters, The urban land and roads in the study area are mostly distributed in the low altitude area of the region, suggesting that regional debris flow disasters may cause significant damages.

The results of the relationship between debris flow susceptibility and slope (Fig. 11) showed that the range slope with debris flow susceptibility was 0°–75.44°, and the overall distribution was relatively concentrated between 20° and 40°. Below 35°, the percentage of susceptibility areas increases step by step with the increase of slope grade; above 35°, the percentage of susceptibility areas decreases step by step with the increase of slope grade. The medium and high level susceptibility areas are mainly concentrated in the range of slope grades below 40°. This result suggests that the low slope (between 20° and 40°) of the study area provides favorable topographic conditions for the occurrence of debris flow disasters, while higher slopes of the study area are more favorable for low debris susceptibility. In the study area, villages, buildings, and farmland are more distributed in low-sloped areas,



making debris flow more damaging to society and the economy.

The results of the relationship between debris flow susceptibility and flow accumulation (Fig. 12) show that the range of flow accumulation values for debris flow susceptibility is 0–37856056, and the susceptibility is mainly distributed in the range of lower flow accumulation. The higher the flow accumulation, the lower the distribution range of debris flow susceptibility areas, but with a higher flow accumulation, the higher the debris flow susceptibility. Susceptibility values were mainly distributed in the range of low flow accumulation rates. However, the grid unit upstream peripheral convergence may exhibit high cumulants under rainfed conditions, resulting in low debris flow diffusion in this grid and gradual downward diffusion.

The results of the relationship between debris flow susceptibility and plane curvature (Fig. 13) show that the plane curvature of debris flow susceptibility is  $-21.822/100\text{ m}^{-1}$  to  $20.257/100\text{ m}^{-1}$ , and the distribution of debris flow susceptibility is relatively concentrated in the plane curvature of  $-2/100\text{ m}^{-1}$  to  $1/100\text{ m}^{-1}$ , among which the medium to high susceptibility is mainly distributed at  $-2/100\text{ m}^{-1}$  to  $0/100\text{ m}^{-1}$ . This indicates that the study area The plane curvature of  $-2/100\text{ m}^{-1}$  to  $1/100\text{ m}^{-1}$  in the study area provides more favorable topographic conditions for debris flow spreading and propagation. The debris flow downstream accumulation area is more distributed within the concave terrain with negative values of  $-2/100\text{ m}^{-1}$  to  $0/100\text{ m}^{-1}$ , and the medium to high susceptibility is more easily formed by diffuse accumulation and damage to the downstream.

Land use types were extracted by masking in Arcgis software using susceptibility results, and then susceptibility ratios were calculated for each land use type (Fig. 14). The susceptibility areas of cultivated land accounted for 20.00%, with an average susceptibility value of 0.1478. In addition, the proportion values of susceptibility areas in woodland, grassland, water, unused, and building lands were 20.61, 14.22, 1.09, 38.15, and 5.93%, with average values of 0.1349, 0.1185, 0.1402, 0.1054, and 0.1068, respectively. The debris-flow susceptibility areas were abundant in the unused land and less prevalent in the water area. In addition, the highest and lowest susceptibility values were observed in cultivated and unused lands, respectively. It should be noted that the proportion of building lands in the study area is not high (about 6%), but the proportion of building lands with susceptibility reaches nearly 6% of the susceptibility types, indicating that the distribution range of debris flow susceptibility on building lands is high and can have far-reaching effects on human activities in the area.

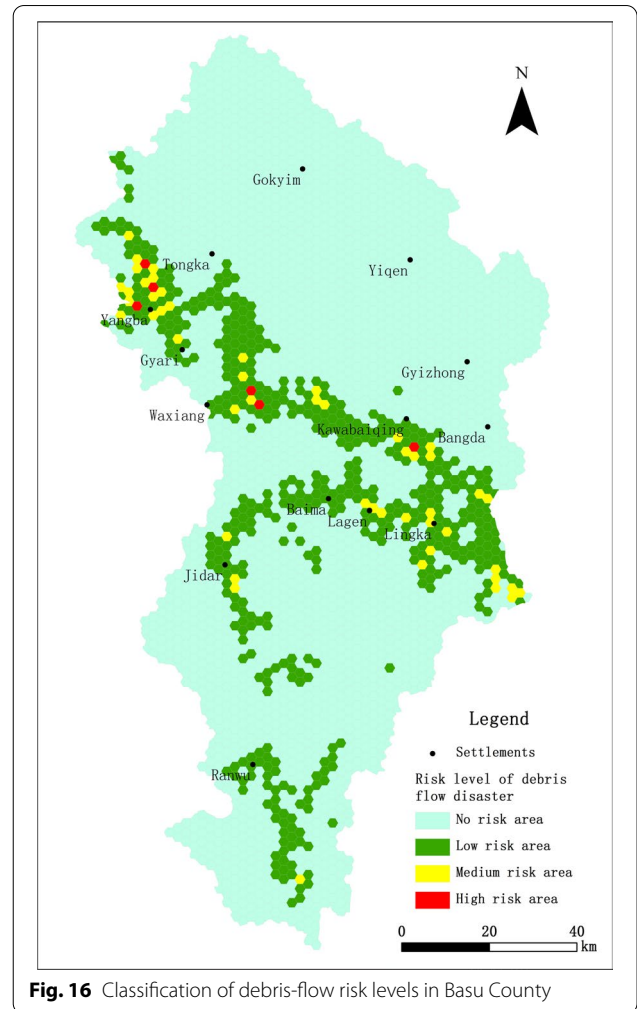


**Fig. 16** Classification of debris-flow risk levels in Basu County

**Debris flow disaster risk assessment**

The vector risk exposure body information obtained from OpenStreetMap was rasterized using ArcGIS software, with a data resolution of 12.5 m, to ensure that each pixel of the grid is aligned with the susceptibility result pixels obtained by the Flow-R model, the area of the exposure body in the region is about 34.07km<sup>2</sup>, and building area in the study area is relatively small and concentrated, and the main exposeure bodies are roads. The overlap between the risk exposure body map and the susceptibility result of debris flow refers to the risk exposure body with high vulnerability located in the debris-flow susceptibility area. The area and extent of potentially exposed to debris flow disaster risk were determined (Fig. 15).

The debris flow disaster risk in the region can be obtained by identifying the debris flow susceptibility areas that are prone to high property losses and vulnerability to disaster. The potential risk areas of debris flow disaster in the study area are mostly located on roads, covering a total area of about 0.82 km<sup>2</sup>. The potential

debris flow risk areas accounted for 0.84% of the total surface of debris-flow susceptibility. In addition, the area of low-susceptibility, medium-susceptibility, and high-susceptibility risks were about 0.64 and 0.14, and 0.04 km<sup>2</sup>, respectively. These results indicate that this method can reduce the extent of debris flow disaster monitoring and warning, target specific areas of the road and building before planned reinforcement, and allows disaster prevention measures, thus reducing the economic loss caused by debris flow disaster.

### Disaster risk zoning

The risk levels of debris flow in the study area were classified based on the risk of debris flow on a unit grid. Several regular hexagonal grids, with a unit area of 4 km<sup>2</sup>, were established using Generate Tessellation tool in ArcGIS software, while the small marginal areas (less than 2 km<sup>2</sup>) were eliminated. The study area is large, and when the unit area is selected, too small will lead to overly fragmented division results, and too large will lead to difficulty reflecting the differences in the region. After comprehensive consideration and comparison, 4km<sup>2</sup> was finally chosen as the unit area. The regular hexagon is closer to the circle than the regular quadrilateral, exhibiting a smaller area/circumference ratio. Indeed, the regular hexagon is a similarly shaped polygon that can be arranged uniformly in space, thus significantly minimizing the result deviation caused by the boundary effect and better reflecting the internal information and condition of regional space. The sum of debris flow risk in each hexagonal grid was calculated before classifying the regional debris flow risk level in the same unit area. The susceptibility values were superimposed on each unit area and the results ranged from 0 to 881.9858, the susceptibility values per unit area were equal interval method classified into four classes, namely no risk (0), low risk (0–300), medium risk (300–600), and high risk (600–900). The potential disaster risk was visualized to reveal the spatial variation of debris flow risk in the study area (Fig. 16).

The debris flow risk map revealed 3 082 regional disaster risk level grids, including 2 534, 493, 49, and 6 grids showing no risk, low risk, medium risk, and high risk areas, respectively. Therefore, most parts of the study area have exhibited no debris flow risk. Moreover, most debris flow risk areas are of low risk, while the areas of medium and high debris flow risks are small and spatially scattered.

According to the results of risk zoning, it is necessary to improve strategies to prevent regional debris flow disasters, particularly in areas presenting medium to high susceptibility areas of debris flow disaster, and reduce human activities in susceptible areas to effectively

prevent and mitigate debris flow hazards. In risk-free areas, there is generally no risk of debris flow disaster. Human activities can, therefore, be carried out normally. Investment in disaster prevention and control in the non-risk areas can be moderately reduced, thus allowing additional disaster prevention and control resources to be allocated to areas of high debris flow risk. Human activities can also be carried out in low-risk areas, but it is necessary to strengthen disaster warning and detection in areas of low debris flow risk and appropriately invest in disaster prevention and mitigation forces. In medium risk areas, artificial construction facilities and agricultural activities need to be reduced, and existing facilities and buildings should be strengthened and relocated to reduce the risk of debris flow disaster, improve the awareness of disaster prevention among regional residents, strengthen the level of disaster warning and monitoring, and continuously detect regional disaster risk. In high-risk areas, it is suggested to avoid the construction of artificial facilities and relocate the existing facilities and residential areas, and strengthen resource investment in effective reinforcement management of roads in the study area, to reduce disaster losses.

The above suggestions can effectively reduce and control the regional debris flow disaster, improve the level of debris flow warning, particularly in the rainy season, enhance disaster risk forecasting, implement disaster prevention and mitigation related works, thus effectively reducing the risk of life and property safety caused by debris flow disaster in Basu County.

### Discussion

It is difficult to accomplish high-resolution susceptibility identification at the regional scale, so the Flow-R model, a method in which a small amount of data can quickly obtain more accurate results, is used to identify the potential spread of debris flow at the regional scale. Because the susceptibility results of the Flow-R model are constrained by the quality of DEM, so in the range of 12300km<sup>2</sup>, we choose 12.5 m resolution on the basis of not destroying the original data resolution, considering the data accessibility and model operation, to obtain the highest possible data resolution and susceptibility result quality. Of course, the model is limited and does not reflect the local control factors and specific conditions. The results are often larger than the actual extent of debris flow occurrence, but the output can be considered accurate for the purpose of susceptibility mapping (Horton et al. 2011).

The validation of the results is an important reflection of the accuracy and validity of the model. In this paper, the results are validated based on the disaster points list and the visual comparison of remote sensing images,

and the accuracy of the validation points reaches 87.6%. According to the comparison of remote sensing images, the debris flow channels in the susceptibility area have obvious characteristics, and the overall results of the model in the study area are ideal, and the results have a high degree of confidence. However, for the accurate portrayal of the debris flow extent for validation, this paper obviously did not do enough. Due to the limitation of image quality and technical level, the actual occurrence of regional large scale debris flow is difficult to obtain. Because it is difficult to extract debris flow extent information directly from the images, firstly, the rainfall is concentrated before and after the occurrence of debris flow and the cloud cover is large, so the real images are not easy to obtain. Moreover, the debris flow accumulation will be covered by the natural changes of the ground surface with time changes, so it is often impossible to directly obtain the actual location of debris flow occurrence, and the remote sensing image resolution itself has some limitations on the results. Due to the difference of natural conditions on a regional scale, the texture features and so on of debris flow are not consistent on the images of different regions. Remote sensing interpretation of debris flow information on a large scale is obviously more difficult, but the validation of a small scale single debris flow ditch can be carried out by overlaying research results with images if high-resolution images can be obtained, and such validation can only be carried out after the occurrence of a disaster, which is undesirable in areas with frequent human activities. Therefore, the debris flow risk in the region can be effectively estimated before disasters occur, providing references for debris flow prevention and control policies, specific regional construction planning, as well as disaster prediction and early warning systems, thus reducing financial and economic losses and protecting people's lives.

Debris flow hazards are influenced by the complex surrounding environment, and the uncertainty of regional scale data and the model itself is inevitable, meanwhile, there must be errors between such nonlinear research analysis and the actual situation, and it is often necessary to make a lot of adjustment work on parameters to compare with the actual local occurrence to reduce simulation errors. Some algorithms in the Flow-R model are mainly derived from empirical algorithms, explaining the multiple different choices that have been made in terms of method and parameter considered in the model. Horton et al. (2013), Kang and Lee (2018), and Park et al. (2016), compared different data resolutions, methods, and parameters, compared the susceptibility values and ranges under different parameter configurations, and explored the most reasonable values of parameters in different regions. In this study, the debris flow disaster in

the study area was assessed at on a large scale. The results of this study were not compared and discussed by adjusting data resolution, model methods, and parameters due to the running time of the model, but by referring to the parameter selection in related studies. The susceptibility acquisition based on Flow-R is characterized by easy access to data, relatively reliable results (according to the comparison and validation of this paper), high resolution of results (generally large scale results are difficult to apply to road risk evaluation, and the roads in this study area are critical), and the ability to distinguish local scale debris flow susceptibility changes, based on which regional scale risk evaluation is conducted, and susceptibility information extraction based on regional debris flow related. Although there may be some deviations between the results and the actual situation, the large scale high-resolution results can be applied to the overall regional risk assessment and zoning, so that the high susceptibility and risk areas can be prevented in advance.

## Conclusions

In this study, the 12.5 m resolution DEM data were used in the Flow-R model to identify the regional debris flow susceptibility. The results were first validated using the actual disaster point data combined with remote sensing images, and then the regional disaster risk was further evaluated. The main conclusions reached are follows:

(1) There was a lack of susceptible debris flow areas in most parts of the study area. The debris flow susceptibility areas were mainly observed in the Nujiang River valley, the tributaries of the Lengqu river, and both sides of National Highway 318, covering a total area of about 97.04 km<sup>2</sup> (0.79% of the study area). Moreover, low, medium, and high susceptibility areas covered 0.59, 0.15, and 0.05% of the study area, respectively. In the Nujiang River valley, the debris flow susceptibility was more widely distributed than that along National Highway 318. Although the high susceptibility value of debris flow are prone to disasters, their area may be small. These areas were distributed along the valley channel. The debris flow in the low susceptibility zone is not easy to occur but has a greater range and extends around the channel, depending on the terrain characteristics.

(2) The debris flow susceptibility in the study area was mainly distributed in areas with altitude values below 4000 m, particularly on both sides of the river valley, at an altitude range of 3000–4000 m. In addition, the results revealed the distribution of the susceptibility values within the low-slope range of 20–40°, thus providing favorable terrain conditions for the occurrence of debris flow disasters. The susceptibility is mainly distributed in the range where the flow accumulation is low, and the higher the flow accumulation, the higher the range of

debris flow susceptibility distribution is about less, but with the higher flow accumulation, the debris flow susceptibility is much higher. The areas with plane curvature from  $-2/100$  to  $1/100 \text{ m}^{-1}$  were more susceptible to debris flow, providing favorable terrain conditions for debris flow diffusion. On the other hand, the debris flow susceptibility areas were most abundant in the unused land and less prevalent in the water area. In addition, the highest and lowest susceptibility values were found in cultivated and unused lands, respectively.

(3) The risk exposure body such as buildings, residential areas and roads in the susceptible areas was employed to determine the potential debris flow disaster risk. Most of the risk exposure bodies were located on the road surface, covering a total area of  $0.82 \text{ km}^2$  (0.84% of debris-flow susceptibility areas). The risk level of the study area was classified, taking into account  $4 \text{ km}^2$  as a unit area. The results revealed a low overall debris flow risk level in the study area, with few and scattered areas of medium–high risk.

#### Acknowledgements

This work was supported by Second Tibetan Plateau Scientific Expedition and Research Program (STEP) [Grant No. 2019QZKK0906] and China's National Key Research and Development Project (NKPs) [Grant No. 2019YFA0606902].

#### Author contributions

Huang Xu and Peng Su designed this study in consultation with Qiong Chen, Huang Xu handled the analysis of the data and completed the manuscript with the support of other authors. All authors read and approved the final manuscript.

#### Funding

This work was supported by Second Tibetan Plateau Scientific Expedition and Research Program (STEP) [Grant No. 2019QZKK0906] and China's National Key Research and Development Project (NKPs) [Grant No. 2019YFA0606902].

#### Availability of data and materials

All data and materials are available from the corresponding author upon reasonable request.

#### Declarations

#### Competing interests

The authors declare that they have no competing interests.

#### Author details

<sup>1</sup>College of Geographic Sciences, Qinghai Normal University, Xining 810008, China. <sup>2</sup>Academy of Plateau Science and Sustainability, Xining 810008, China. <sup>3</sup>Institute of Geographic Sciences and Natural Resources Research, CAS, Beijing 100101, China.

Received: 23 March 2022 Accepted: 1 June 2022

Published online: 06 June 2022

#### References

- Baumann V, Wick E, Horton P, Jaboyedoff M (2011) Debris flow susceptibility mapping at a regional scale along the National Road N7, Argentina. In: Proceedings of the 14th Pan-American conference on soil mechanics and geotechnical engineering, Canadian Geotechnical Society, 2011: 2–6
- Bian JH, Li XZ, Hu KH (2018) Study on distribution characteristics and dynamic evolution of mountain hazards in Hengduan mountains area. In: China engineering geology annual conference on 2018. Xi'an 2018
- Blahut J, Horton P, Sterlacchini S, Jaboyedoff M (2010) Debris flow hazard modelling on medium scale: Valtellina di Tirano, Italy. *Nat Hazard* 10(11):2379–2390
- Blais-Stevens A, Behnia P (2016) Debris flow susceptibility mapping using a qualitative heuristic method and Flow-R along the Yukon Alaska Highway Corridor, Canada. *Nat Hazard* 16(2):449–462
- Cama M, Lombardo L, Conoscenti C, Rotigliano E (2017) Improving transferability strategies for debris flow susceptibility assessment: application to the Saponara and Itala catchments (Messina, Italy). *Geomorphology* 288:52–65
- Chen HK, Tang HM (2011) Evaluation of geological disaster fatality along Sichuan–Tibet highway. *Chin Highw* 09:17–23
- Cui P, Liu SJ, Tan WP (2000) Progress of debris flow forecast in China. *Chin J Nat Disasters* 02:10–15
- Cui P, Su FH, Zou Q, Chen NS, Zhang YL (2015) Risk assessment and disaster reduction strategies for mountainous and meteorological hazards in Tibetan Plateau. *Chin Sci Bull* 60(32):3067–3077
- Cui P, Guo XJ, Jiang TH, Zhang GT, Jin W (2019) Disaster effect induced by Asian water tower change and mitigation strategies. *Bull Chin Acad Sci* 34(11):1313–1321
- Dowling CA, Santi PM (2014) Debris flows and their toll on human life: a global analysis of debris-flow fatalities from 1950 to 2011. *Nat Hazards* 71(1):203–227
- Fell R, Corominas J, Bonnard C, Cascini L, Leroi E, Savage WZ (2008) Guidelines for landslide susceptibility, hazard and risk zoning for land-use planning. *Eng Geol* 102(3–4):99–111
- Gomes RAT, Guimarães RF, De Carvalho J, Fernandes NF, Do Amaral J (2013) Combining spatial models for shallow landslides and debris-flows prediction. *Remote Sens* 5(5):2219–2237
- Gong K, Yang T, Xia C, Yang Y (2017) Assessment on the hazard of debris flow based on FLO - 2D: a case study of debris flow in Cutou Gully, Wenchuan, Sichuan. *Chin J Water Resour Water Eng* 28(06):134–138
- Gong P, Liu H, Zhang M et al (2019) Stable classification with limited sample: transferring a 30-m resolution sample set collected in 2015 to mapping 10-m resolution global land cover in 2017. *Sci Bull* 64(6):370–373
- Horton P, Jaboyedoff M, Zimmermann M, Mazottf B, Longchamp C (2011) Flow-R, a model for debris flow susceptibility mapping at a regional scale—some case studies. *Ital J Eng Geol* 2:875–884
- Horton P, Jaboyedoff M, Rudaz B, Zimmermann M (2013) Flow-R, a model for susceptibility mapping of debris flows and other gravitational hazards at a regional scale. *Nat Hazards* 13(4):869–885
- Horton P, Jaboyedoff M, Bardou E (2008) Debris flow susceptibility mapping at a regional scale. In: Proceedings of the 4th Canadian Conference on Geohazards: From Causes to Management. Presse de l'Université Laval, Québec
- Hou YL, Hu SJ, Peng QY, Xu JK, Wu XG (2019) Analysis of debris flow susceptibility in loess gully region: a case study of Laolang Gully in Lanzhou. *Chin Ecol Environ Monit Three Gorges* 4(04):48–56
- Hu XY, Qin SW, Dou Q, Liu F, Qiao SS, Dong D (2019) Susceptibility analysis of debris flow based on GIS and random forest—a case study of a mountainous area in northern Taonan City, Jilin Province. *Chin Bull Soil Water Conserv* 39:204–210
- Iverson RM (1997) The physics of debris flows. *Rev Geophys* 35(3):245–296
- Kang S, Lee S (2018) Debris flow susceptibility assessment based on an empirical approach in the central region of South Korea. *Geomorphology* 308:1–12
- Kritikos T, Davies T (2015) Assessment of rainfall-generated shallow landslide/debris-flow susceptibility and runoff using a GIS-based approach: application to western Southern Alps of New Zealand. *Landslides* 12(6):1051–1075
- LCC Committee of Basu County, Tibet Autonomous Region (2012) Basu County local chronicles. Basu Publishing House, Chengdu ((in Chinese))
- Llanes F (2016) Characterization, critical rainfall, and 2D-numerical modeling of Philippine non-volcanic debris flows from the December 2015 Typhoon Melor event. In: AGU Fall Meeting Abstracts (Vol. 2016, pp. EP21C-0892)
- Luo DF, Mao JZ, Zhu PY et al (1996) Mountain disasters and prevention countermeasures on south Line of Sichuan–Tibet Highway (in Tibet). Science Press, Beijing ((in Chinese))

- Lv RR et al (1999) Debris flow and environment in Tibet. Chengdu University of Science and Technology Press, Chengdu ((in Chinese))
- Nie YP, Li XZ (2019) Hazard assessment of Bayi Gully debris flow based on Flow-R model. *Chin J Nat Disasters* 28(01):156–164
- Park DW, Lee SR, Vasu NN, Kang SH, Park JY (2016) Coupled model for simulation of landslides and debris flows at local scale. *Nat Hazards* 81(3):1653–1682
- Pastorello R, Michelini T, D'Agostino V (2017) On the criteria to create a susceptibility map to debris flow at a regional scale using Flow-R. *J Mt Sci* 14(4):621–635
- Qing F, Zhao Y, Meng X, Su X, Qi T, Yue D (2020) Application of machine learning to debris flow susceptibility mapping along the China–Pakistan Karakoram Highway. *Remote Sens* 12(18):2933
- Rickenmann D, Zimmermann M (1993) The 1987 debris flows in Switzerland: documentation and analysis. *Geomorphology* 8(2–3):175–189
- Shi PJ (2018) *Disaster risk science*. Springer, Berlin ((in Chinese))
- Sturzenegger M, Holm K, Lau C, Jakob M (2019) Semi-automated regional scale debris-flow and debris-flood susceptibility mapping based on digital elevation model metrics and Flow-R software. Proceedings of the Seventh International Conference on Debris-Flow Hazards Mitigation, Golden, Colorado, USA
- Takahashi T (1981) Estimation of potential debris flows and their hazardous zones: soft countermeasures for a disaster. *Nat Disaster Sci* 3(1):57–89
- Tang C, Liang JT (2008) Characteristics of debris flows in Beichuan epicenter of the Wenchuan earthquake triggered by rainstorm on September 24. *Chin J Eng Geol* 16(06):751–758
- Wang Y, Tang C, Li WL, He C (2017) Application of GIS-based fuzzy mathematics model to sensitivity evaluation of debris flow. *Chin J Nat Disasters* 26(01):19–26
- Wu S, Chen J, Zhou W, Lqbal J, Yao L (2019) A modified Logit model for assessment and validation of debris-flow susceptibility. *Bull Eng Geol Env* 78(6):4421–4438
- Xia CH, Zhu J, Chang M, Yang Y (2017) Susceptibility assessment of debris flow using a probabilistic and GIS approach: a case study on the Wenchuan county. *Chin J Yangtze River Sci Res Inst* 34(10):34–38
- Xie XJ, Wei FQ (2011) Study on fractal dimension and stability of land use types in the area with High-frequency debris flow. *Chin Res Soil Water Conserv* 18(6):167–176
- Xiong K, Adhikari BR, Stamatopoulos CA, Zhan Y, Wu S, Dong Z, Di B (2020) Comparison of different machine learning methods for debris flow susceptibility mapping: a case study in the Sichuan Province, China. *Remote Sens* 12(2):295
- Xu W, Yu W, Jing S, Zhang G, Huang J (2013) Debris flow susceptibility assessment by GIS and information value model in a large-scale region, Sichuan Province (China). *Nat Hazards* 65(3):1379–1392
- Yang QC, Yuan GX, Gao A (2012) Measures for controlling debris slopes and their effects along the Basu to Linzhi section of Sichuan-Tibet highway. *Chin J Geol Hazards Environ Preserv* 23(04):41–45
- Zhang Y, Ge T, Tian W, Liou Y (2019) Debris flow susceptibility mapping using machine-learning techniques in Shigatse area, China. *Remote Sens* 11(23):2801
- Zou Q, Cui P, Yang W (2013) Hazard assessment of debris flows along G318 Sichuan-Tibet highway. *Chin J Mt Sci* 31(03):342–348

## Publisher's Note

Springer Nature remains neutral with regard to jurisdictional claims in published maps and institutional affiliations.

Submit your manuscript to a SpringerOpen<sup>®</sup> journal and benefit from:

- Convenient online submission
- Rigorous peer review
- Open access: articles freely available online
- High visibility within the field
- Retaining the copyright to your article

---

Submit your next manuscript at ► [springeropen.com](https://www.springeropen.com)

---